Case Studies in Construction Materials 23 (2025) e05636

Contents lists available at ScienceDirect

Case Studies in Construction Materials

journal homepage: www.elsevier.com/locate/cscm

Case study

Mechanical characterisation of a two-component grout for tunnel construction

Lucia Mele [a], Carmine Todaro [b,*], Emilio Bilotta [a], Daniele Peila [b]

[a] Department of Civil, Architectural and Environmental Engineering, University of Naples Federico II, Naples 80125, Italy
[b] DIATI, Department of Environment, Land and Infrastructure Engineering, Politecnico di Torino, Corso Duca degli Abruzzi 24, Torino 10129, Italy

ARTICLE INFO

Keywords:
Shield TBMs
Two-component grout
Oedometric modulus
Triaxial test
Effective cohesion

ABSTRACT

Two-component grout (2CG) is the most popular technology for the backfilling phase when shield machines are used for tunnelling. Despite its intensive use, however, its mechanical behaviour has not yet been studied in depth, and there is a need for more knowledge due to the complex numerical models used by designers for mechanised tunnelling projects. In this paper, the results of a laboratory test campaign based on one-dimensional and triaxial compression tests are reported and discussed. Different curing times were tested in an oedometer with varying pre-loads, and the outcomes highlighted the role played by the pre-load in terms of improving the stiffness of the grout, particularly when applied at the early stages of curing. Triaxial tests have never been carried out on 2CG and this paper reports the first obtained outcomes. Tests performed on a ripe material (curing time higher than 28 days) provided values for the effective cohesion (c') and friction angle (φ') that were compared to values in the scientific literature obtained from direct shear tests. A further innovation of the work is the promising attempt to interpret the experimental mechanical behaviour of 2CG in the framework of critical state soil mechanics (CSSM).

1. Introduction

In recent decades, the use of a shield machine for tunnelling construction has been growing. Regardless of the specific technology used by the shield machine (such as an earth pressure balance (EPB) machine, slurry machine, shield rock TBM), the backfilling phase has been shown to be crucial for the correct construction of a tunnel, since it is only by properly filling the annular gap that surface subsidence and lining movements can be avoided. The backfilling phase cannot be avoided due to the nature of the shield technology, as the outer diameter of the assembled lining is smaller than the inner diameter of the shield, and this peculiarity allows for the assembly of the lining under the protection of the shield. This geometrical difference can be computed as the sum of the shield thickness, the tail brush clearance, and the additional gap produced by the conicity of the shield, the larger size of the cutting wheel, and the unavoidable pitching, yawing and rolling of the TBM. Hence, an annular gap of a few centimetres is continuously created during the advancement of the machine, which is also known as an "annulus" (Fig. 1).

Of the available technologies for backfilling, two-component grout (2CG) is the most widely used due to its unquestionable operative and technical advantages [2]. This technology is based on two fluids that are physically and chemically stable and that can be pumped from the bathing station (commonly located in the yard of the construction site) directly to the machine, without the need for intermediate boosting stations, along two separate lines. Component A is typically a cement-based material made up of water, cement,

* Corresponding author.
E-mail address: carmine.todaro@polito.it (C. Todaro).

https://doi.org/10.1016/j.cscm.2025.e05636
Received 31 July 2025; Received in revised form 13 November 2025; Accepted 1 December 2025
Available online 4 December 2025

a retarding-fluidifying agent and bentonite. Further ingredients are also used for the production of component A in order to optimise the performance of the grout and the cement dosage, such as granulate blast furnace slag, fly ash and metakaolin [3,4]. Component B is a solution of sodium silicate, known as the "accelerator". Both fluids remain stable until the turbulent mixing phase, which occurs a few centimetres before the injection nozzles. Nozzles are deployed circumferentially on the shield's tail and provide the injection flow to the annulus during advancement of the machine.

Each ingredient of the grout plays an important role, and the mix design is the result of a laboratory test campaign that is tailored to ensure compliance of the grout with the design requirements. The standard testing procedure is based on measurements of the unit weight, bleeding and fluidity of component A (to assess its homogeneity, physical stability and chemical stability, respectively), with tests of the gelling time of the two components and their mechanical properties. In the last group of tests, the short-term surface compression strength (SCS) is assessed within 3 h from the time of grout gelation, whereas the uniaxial compression strength (UCS) is the main parameter used for characterisation after one day [5,6]. However, it is worth noting that other mechanical parameters are increasingly required at the design stage to model the elastic-plastic behaviour of the grout for numerical analyses, such as the elastic moduli [7], the Mohr–Coulomb shear strength parameters (i.e. cohesion and friction angle), and the permeability coefficient.

Despite its widespread use, however, knowledge of its hydraulic and mechanical properties, their evolution over time and the effect on their long term performance of any external loads that may be applied to them while curing (for example, due to the installation of a new lining ring or the passage of the machine backup) is scant. It is also difficult to characterise 2CG with reliable methods, since standard approaches are often not directly applicable due to the fast transformation that affects the grout (with a transformation rate that is not constant in time, and is faster in the first hours and slower after some days). Although at first glance this peculiarity appears to present a problem, this paper describes a method of taking advantage of this process to improve the quality of the material. For this purpose, a specific experimental campaign was carried out in the laboratory, consisting of one-dimensional compression and triaxial compression tests.

One-dimensional (oedometric) compression tests were conducted to investigate the potentially beneficial effect of the pre-loading applied to the material, which allowed for the assessment of the permeability coefficient of the 2CG (k). The evidence indicates that if a certain pre-load is applied to a grout specimen before applying the typical load sequence, the grout exhibits increased oedometric stiffness (E_{oed}). The potential benefits that can be achieved are also dependent on the curing time, since for a given value of the pre-load, the "fresher" the sample at the time of pre-loading, the higher the final E_{oed}.

To the best of our knowledge, triaxial tests have not previously been carried out on 2CG specimens. Their outcomes, in terms of the cohesion (c') and friction angle (φ') characterising the Mohr–Coulomb failure criterion, are compared to the same parameters obtained for a grout with the same mix design through a direct shear test [8]. The second part of the paper highlights the complexity involved in characterising 2CG and the influence that the procedure itself could have on the final result. We note that experimental data obtained from triaxial tests can be interpreted in the light of critical state soil mechanics, and that despite 28 days of curing, the material does not completely lose its original nature (similarly to a cemented clay rather than a concrete).

Before to proceed with the reading, it should be always considered that at the real scale of the machine, 2CG is produced and injected in quantities of several cubic metres per thrust, and that as a consequence, the real mechanical properties of the backfilling material could differ from those computed at the laboratory scale. However, the data reported in this paper remain of great importance and can be considered as reference points for numerical models or further investigations.

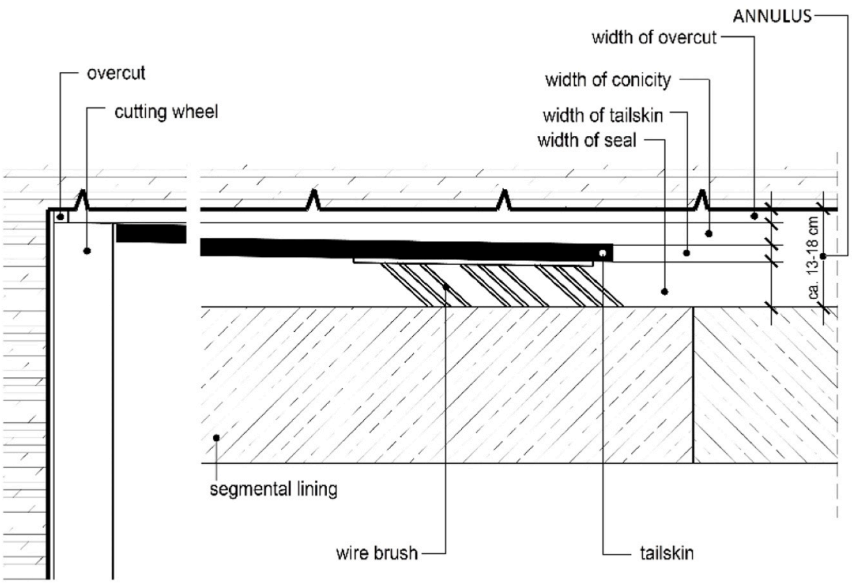

Fig. 1. Schematic diagram of the annulus (modified from [1]).

2. Material, methods and testing program

2.1. Material used

The material representing component A in this work is a standard one made up of cement, bentonite, a retarding/fluidifying agent and water. Portland Cement type CEM I 52.5 R was used, while the bentonite was a sodic type. Details of the assessment of the swell index (SWI), smectite content and unit weight of the used bentonite can be found in [7] with reference to bentonite type 1.

The water was taken from the municipal water network of Naples (Italy), while the chemicals (accelerator and retarding/fluidifying agent) were supplied by Mapei.

2.2. Production of component A and sample casting

Component A was produced according to the procedure described in [5], as summarised in Table 1. Bentonite, cement and the retarding/fluidifying agent were added to the water in sequence, and were thoroughly stirred with a laboratory mixer equipped with a proper blade. Details of the dosages for the mixture can be found in Table 2.

Components A and B were mixed according to the procedure described in [6]. The blend was then poured into suitable standard moulds (Fig. 2) before quick gelation (in less than 10 s).

The specific gravity of the resulting grout was calculated following the standard procedure reported in [9], with a resulting value of 26.96 kN/m^3.

2.3. Testing program

To characterise the mechanical behaviour of the 2CG, oedometer and triaxial tests were conducted. The oedometer tests were performed following [10], using cylindrical moulds 56 mm in diameter and 20 mm in height. The aim of these tests was to investigate the behaviour of the grout under different curing times and varying levels of confining stress. The specimens were loaded and unloaded according to the scheme proposed in [11], and five curing times were considered, according to the following specifications:

– *Zero curing*: Three specimens were loaded according to the standard oedometer incremental loading procedure from 10 to 5000 kPa in 11 steps, except for Oed1_0_0 test, which was loaded up 800 kPa. The specimens were then unloaded to 10 kPa in 11 steps. The aim of these tests was to check repeatability;
– *Curing for 1 h*: Three new specimens were loaded and unloaded at specific vertical stresses of 100, 1200, and 2500 kPa. The loading phase lasted approximately 20 min, to match the corresponding curing duration, followed by unloading over another 20 min. The specimens were subsequently loaded from 10 to 5000 kPa in 11 steps, and then unloaded to 10 kPa in 11 steps, following the procedure for specimens with zero curing time. We note that the specimen loaded at 2500 kPa collapsed when the vertical load was applied;
– *Curing for 24 h*: Two new specimens underwent the same procedure as described above, and were loaded and unloaded at 100 and 2500 kPa. They were then subjected to the procedure followed for specimens with zero curing time;
– *Curing for 7 days*: One new specimen was loaded to 2500 kPa and then unloaded to 0 kPa, following the same procedure used for specimens with zero curing time;
– *Curing for 28 days*: One new specimen was loaded to 5000 kPa and unloaded to 10 kPa, following the same procedure as for specimens with zero curing time.

Triaxial tests were performed according to [12], using moulds 38 mm in diameter and 76 mm in height. These tests were performed on specimens with a curing time exceeding 28 days, in order to assess the strength of grout once it had fully matured (Fig. 3). Saturated specimens were isotropically consolidated by applying a back-pressure (bp) of 0 kPa and a confining stress, σc, ranging from 100 to 800 kPa, and then effective stresses (σ'c=σc – bp) ranging between 100–800 kPa. Tests are, then sheared in strain-controlled tests in drained conditions. The applied strain rate was 0.015 %/min. The experimental results are discussed in the next section.

Curing times longer than 28 days were not investigated, since this time frame is sufficient for the 2CG to be considered ripe [13] and construction site technical specifications do not generally require investigations of curing times of longer than 28 days.

For completeness, it should be reported that the uniaxial compression strength of 2CG has been previously studied and outcomes are available in [5,6].

Table 1
Mixing procedure according to [5].

Phase	Impeller rotation speed (rpm)	Duration (min)
Start (water only)	800	/
Bentonite mixing phase	2000	7
Cement mixing phase	2000	3
Mixing of retarding/fluidifying agent End	2000	2

Table 2
Mix composition.

Ingredient	Dosage (kg/m^3)
Cement - CEM I 52.5 R	230.0
Bentonite	30.0
Retarding/fluidifying agent - Mapequick CBS1	3.5
Accelerating agent - Mapequick CBS3	81.0
Water	851.8

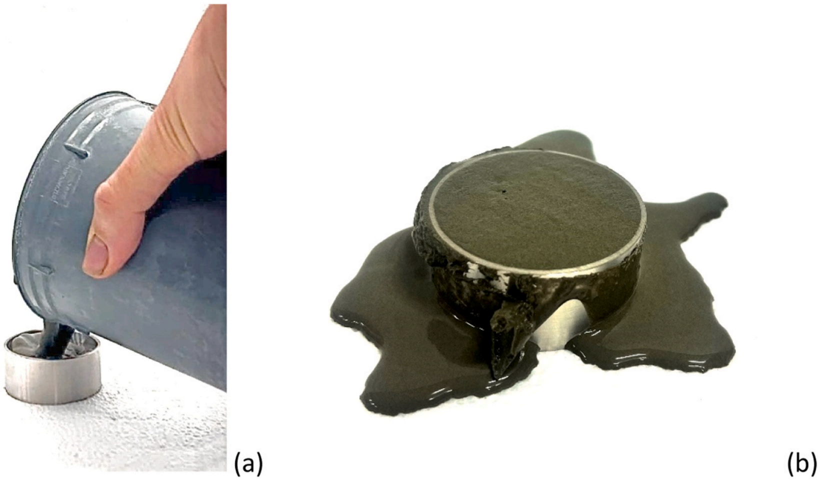

Fig. 2. Oedometer specimen: photographs showing (a) the casting phase and (b) the resulting specimen of two-component grout.

3. Laboratory test results

The main experimental results are presented in this section.

3.1. One-dimensional compression tests

One-dimensional compression tests were performed following the procedure described in the previous section, and the test conditions are summarised in Table 3, where the void ratio (e) is defined as the ratio between the volume of voids (Vv) and the volume of solids (Vs). The latter was determined from the dry weight of the specimens after oven-drying at 105 °C.

In the following the test code Oed_X_YY refers to the curing time (X) and the applied pre-loading (YY, in kPa).

As an example, Fig. 4 shows a plot of the settlement of grout specimens at the pre-loading stage over time. It can be seen that the curves resemble those of natural geomaterials (with an S-shaped curve). The results are therefore interpreted following the main principle of one-dimensional consolidation for soils, although a fundamental difference should be noted in that the grout is still chemically reactive; this means that its water content can change, not only because the pore water can be expelled upon compression (as in geomaterials) but also due to the chemical reactions developing with time, which alter the expected properties at rest. Nevertheless, the classical approach described in [14] is applied to interpret the oedometer tests, in a similar way to [11].

The oedometer deformation of the specimens under preloading is shown in the experimental settlement curves in Fig. 4, and it can be seen that the consolidation process can be considered concluded in the first 20 min, during which the settlement rates are reduced to negligible values. As expected, the results in Fig. 4 show that for a given curing time, specimens subjected to higher pre-loading exhibit higher settlement (see, for instance, Oed_1h_100 vs. Oed_1h_1200, and Oed_24h_100 vs. Oed_24h_2500), and then lower void ratio after pre-loading (e_{post} in Table 3). Furthermore, for a given pre-loading stress, specimens with a higher curing time exhibit lower settlement (see, for instance, Oed_1h_100 vs. Oed_24h_100, and Oed_24h_2500 vs. Oed_7d_2500) and higher e_{post} (Table 3). This is due to the fact that as the curing time approaches 28 days, the material becomes more stable from a chemical point of view, and hence stiffer. For each test sample subjected to pre-loading, the oedometer modulus (E_{oed}) was calculated as the ratio between the applied vertical stress (σ_v) and the vertical strain (ε_z) of the specimen, as reported in Table 3. Fig. 5 illustrates the effect of curing time and vertical pre-loading stress on E_{oed}. Fig. 5(a) shows that there is an increase in E_{oed} with curing time for a lower pre-loading stress (100 kPa), while E_{oed} is roughly constant with curing time at higher stress (2500 kPa). It is also clear from Fig. 5(b) that E_{oed} at 2500 kPa is roughly the same for curing times of 24 h and 7 days. Specimens with lower curing times exhibit a lower oedometric stiffness, in agreement with the results reported in [11] and [15].

For the tests shown in Fig. 4 (with pre-loading), the indirect permeability coefficient (k) was also obtained from the consolidation

Fig. 3. Photograph showing a triaxial specimen of two-component grout.

Table 3
Results of one-dimensional compression tests of two-component grout.

Test	Curing time	e_0 (-)	w (%)	Pre-loading (kPa)	e_{post} (-)	E_{oed}** (MPa)	k** (cm/s)
Oed1_0_0	0	7.165	110	0	7.165	-	-
Oed2_0_0	0	7.493	150	0	7.493	-	-
Oed3_0_0	0	7.451	146	0	7.451	-	-
Oed_1 h_100	1 h	7.645	161	100	6.652	0.9	$3.17 \cdot 10^{-7}$
Oed_1 h_1200	1 h	7.595	111	1200	2.856	2.2	$4.44 \cdot 10^{-8}$
Oed_1h_2500*	1 h	-	-	2500	-	-	-
Oed_24 h_100	24 h	7.628	168	100	7.607	39.9	$3.23 \cdot 10^{-8}$
Oed_24h_2500	24 h	7.678	164	2500	5.201	8.8	$2.61 \cdot 10^{-8}$
Oed_7d_2500	7d	7.530	165	2500	5.525	10.6	$3.30 \cdot 10^{-8}$
Oed_28d_0	28d	7.590	164	0	7.590	-	-

* collapse;
** computed at the pre-loading stage; e_0=initial value of void ratio; w=water content; e_{post}= value of void ratio after pre-loading; E_{oed} = oedometer modulus; k = permeability coefficient.

coefficient c_v, by reversing its definition, as $k = c_v \cdot \gamma_w / E_{oed}$. It is worth noting [11] that the consolidation coefficient c_v can be obtained if certain assumptions are taken into account: (a) the behaviour of the grout during confined loading is similar to that of fine natural granular materials; (b) the interpretation of raw data should follow the one-dimensional consolidation theory; and (c) the Casagrande method of interpreting the rheology of the grout is valid for use in identifying the compressibility features and characteristics of the grout. Based on these assumptions, the values of k are presented in Table 1. The order of magnitude is about 10^{-8} cm/s (with an average value of about 9.06×10^{-8}), regardless of the curing time or the vertical stress applied, results that are in agreement with those presented in [11]. As a final consideration, it can be observed that the tested grout has low permeability parameters over a wide range of operational stresses. It should be specified that k was calculated at the pre-loading stage, where the curves of settlement with time resemble those of geomaterials (Fig. 4). During the subsequent loading stages of the tests, the primary consolidation could not be clearly identified, and the Casagrande method was not applied.

As mentioned in the previous section, all tests were conducted by applying incremental loading up to 5000 kPa (8000 kPa for the

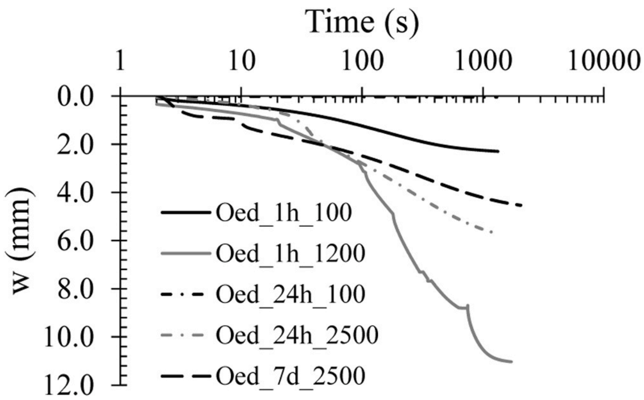

Fig. 4. Settlement of grout over time at the pre-loading stage.

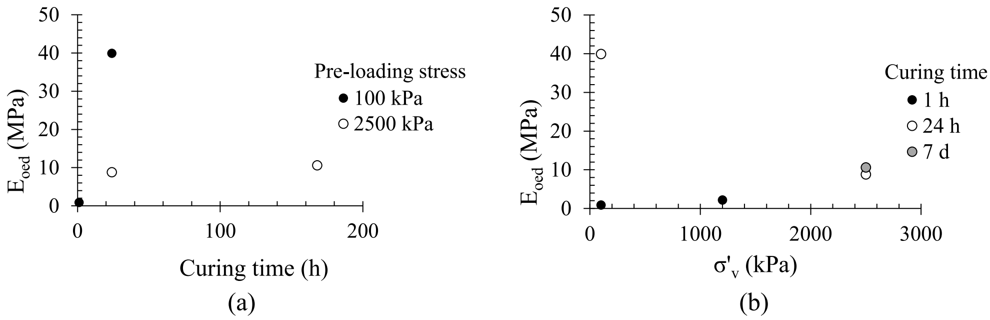

Fig. 5. Changes in oedometer modulus (E_{oed}) with (a) curing time and (b) preloading stress.

Oed1_0_0 test), followed by unloading down to 10 kPa. Throughout the testing process, E_{oed} was calculated at each step of loading and unloading, and the results are displayed in Fig. 6. It should be noted that different axis scales were used to improve the clarity of the graphs and to highlight the differences among the results.The E_{oed} values measured during the loading and unloading stages of the tests, without pre-loading, are compared in Figs. 6(a) and 6(b), respectively. It can be observed that the E_{oed} values measured during loading (Fig. 6(a)) and unloading (Fig. 6(b)) for the Oed1_0_0, Oed2_0_0, and Oed3_0_0 tests are very similar, thus confirming the repeatability of the tests. During the unloading stage, E_{oed} decreases monotonically as the vertical stress decreases. At the loading stage, E_{oed} increases with σ'_v up to 1200 kPa (E_{oed}≈120 MPa), and then suddenly decreases (E_{oed}≈10 MPa).

One interesting outcome is that the Oed_28_0 test shows a lower E_{oed} compared to the other tests, especially during the loading stage (Fig. 6(a)). This apparently contradictory result can be explained by considering the differences in the void ratio. In the first loading step (10 kPa) of the Oed_28_0 test, as expected, the specimen shows a higher E_{oed} (≈2 MPa) compared to the tests with zero curing (E_{oed}≈0.10 MPa). Therefore, the void ratio reached after the first load, e_{10kPa}, is lower in the tests with zero curing (e_{10kPa}≈6.5) than in the Oed_28_0 test (e_{10kPa}≈7.5). Thus, due to its higher void ratio, the specimen from the Oed_28_0 test tends to exhibit lower stiffness in the subsequent loading steps compared to other tests conducted at zero curing time. This result highlights the significant role of void ratio on E_{oed} of 2CG specimens. The E_{oed} values obtained in the pre-loaded tests at the loading stage are plotted in Fig. 6(c), (e), and (g) in function of the σ'_v, showing a bell-shaped curve: E_{oed} increases with the vertical effective stress, reaches a peak, and then decreases. The effective vertical stress at peak increases with the pre-loading stress. For instance, when the Oed_1h_100 and Oed_1h_1200 tests are compared (Fig. 6(c)), we see that in the Oed_1h_1200 test, E_{oed} increases sharply when σ'_v is about 1200 kPa and starts to decrease at the final stage ($\sigma'_v = 5000$ kPa). In contrast, in the Oed_1h_100 test, E_{oed} tends to decrease at 1200 kPa, similarly to the tests with zero curing. Comparable observations can be made for the Oed_24h_100 and Oed_24h_2500 tests (Fig. 6(e)), although in the Oed_24h_100 test, E_{oed} starts to decrease at around 300 kPa.

Although the values of E_{oed} and its behaviour during the loading phase appear to be influenced by curing time or pre-loading, E_{oed} is less affected by these factors in the unloading phase. Indeed, during the unloading phase, E_{oed} is roughly the same across all tests (see Fig. 6(b), (d), (f), and (h)).

The sudden decrease in E_{oed} at the loading stage can be attributed to de-structuring of the grout. To enable a better understanding of this aspect, the test results are plotted in Fig. 7 in the $\sigma'_v - e$ plane.

The experimental results plotted in Figs. 7a and 7(b) (for tests without and with pre-loading, respectively) show that even though the tests start from different void ratios (due to the combined effect of pre-loading and curing time), they converge to a common line, recalling the normal-consolidation line in geomaterials. When this line (shown as a black dashed line in Fig. 7) is reached, the void ratio

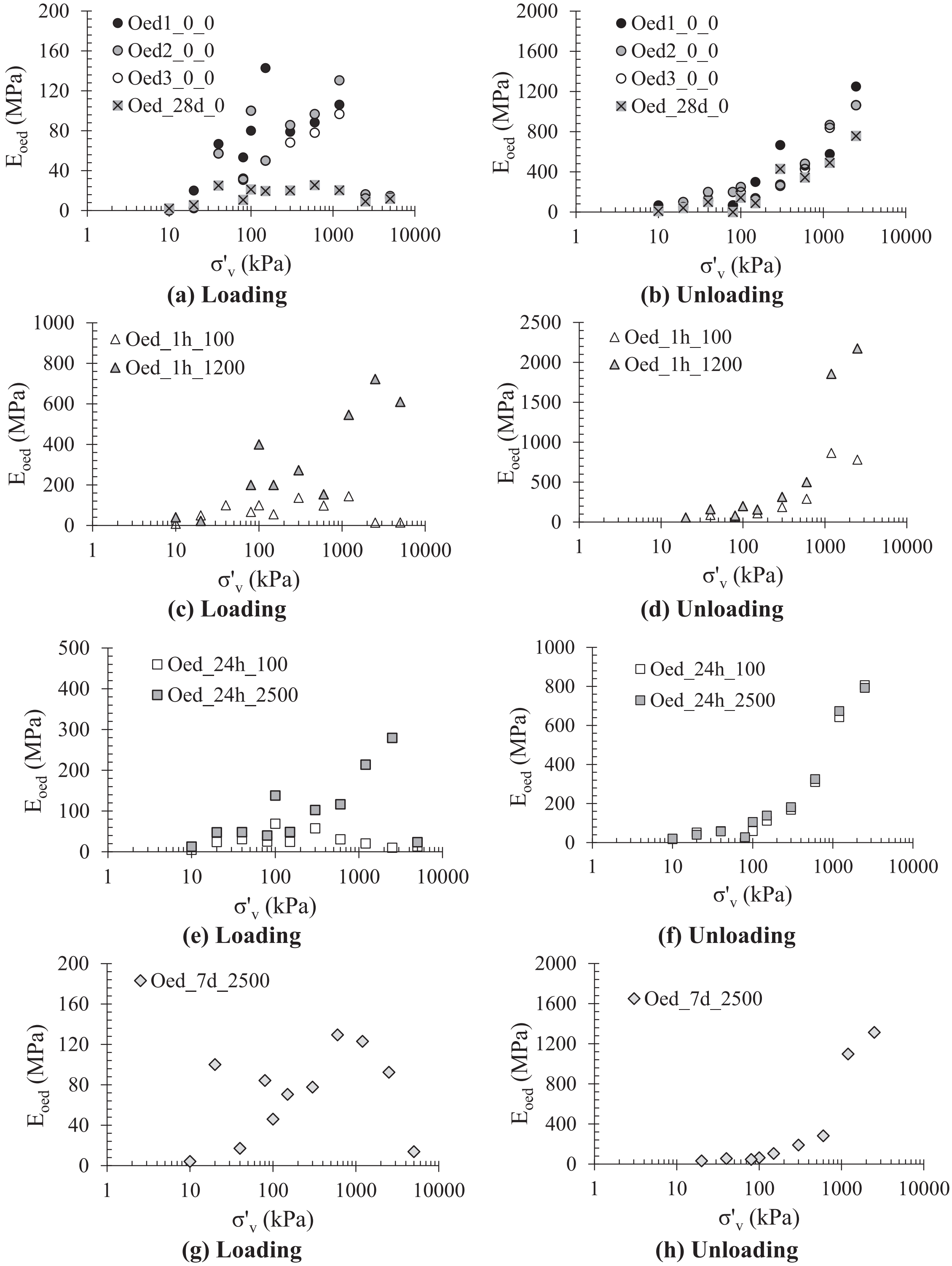

Fig. 6. Changes in oedometer modulus (E_{ed}) with σ'_v in the loading (a-c-e-g) and unloading (b-d-f-h) stages.

decreases sharply, accompanied by a drop in E_{oed} (Fig. 6). This phenomenon is likely to occur because the original structure of the grout breaks down. It can be assumed that cemented bonds start to be destroyed; the line is therefore called the "*deconstruction line*", and has the equation shown in Fig. 7.

This also explains why the observed drop in E_{oed} in Fig. 6 occurs at different values of σ'_v. Specifically, tests with a higher initial void

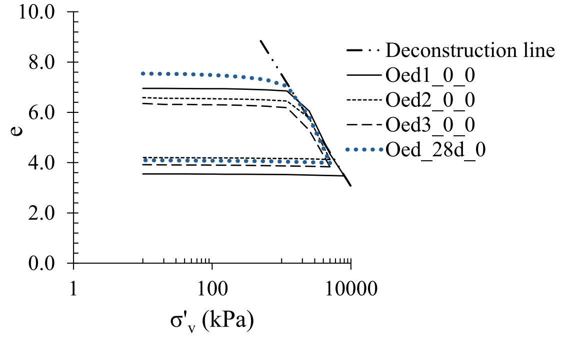

(a)

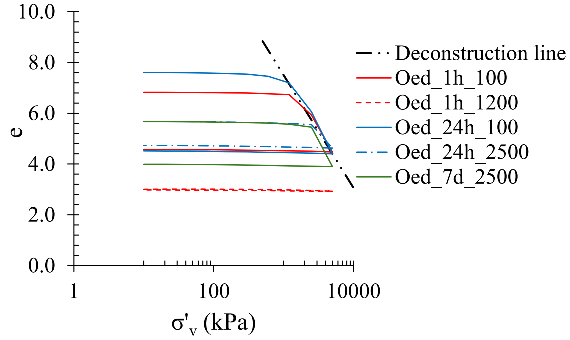

(b)

Fig. 7. Experimental results in the σ'_v – e plane and the deconstruction line for oedometric tests (a) without pre-loading and (b) with pre-loading (b).

ratio (e_{10kPa}) reach the deconstruction line at a lower σ'_v compared to those with a lower e_{10kPa}. For instance, in the Oed_1h_1200 test, where $e_{10kPa} = 3$, a significant drop in E_{oed} is not observed (Fig. 6(c)) because the deconstruction line is not reached.

This suggests that the behaviour of the grout is influenced by the void ratio achieved after the initial load (10 kPa). Hence, early pre-loading of grout after injection can significantly reduce the void ratio and enhance its mechanical properties, for example through an increase in E_{oed}.

The ratio $E_{oed}/E_{oed,0}$ is plotted against e_{10kPa} (Fig. 8) for three different vertical stress levels (80, 300, and 1200 kPa). $E_{oed,0}$ is the oedometer modulus obtained from tests without pre-loading and zero curing time, under a given vertical effective stress (σ'_v). In other words, E_{oed} has been normalised using the average E_{oed} values of tests Oed1_0_0, Oed2_0_0 and Oed3_0_0 at a specific value of σ'_v. Fig. 8 shows a logarithmic relationship between $E_{oed}/E_{oed,0}$ and e_{10kPa}: as e_{10kPa} decreases, the ratio $E_{oed}/E_{oed,0}$ increases. Notably, when e_{10kPa} is approximately three, E_{oed} can be up to five times greater than the value obtained without pre-loading. It can therefore be concluded that the value of e_{10kPa} significantly influences the mechanical behaviour of the grout. If the experimental results are confirmed by other tests, this would mean that the void ratio affects the mechanical behaviour of 2CG more than the curing time.

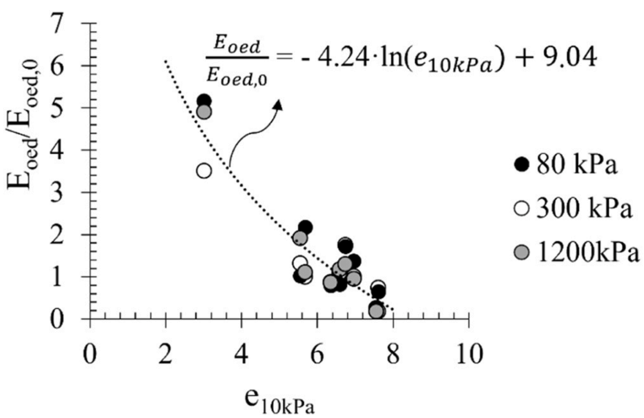

Fig. 8. Relationship between e_{10kPa} and $E_{oed}/E_{oed,0}$ for three vertical stress levels.

Hence, the mechanical behaviour of the tested 2CG crucially depends on its void ratio, as for geomaterials.

3.2. Drained triaxial tests

Five drained triaxial tests were performed on grout specimens with a curing period exceeding 28 days to evaluate their strength once fully matured. The test conditions are detailed in Table 4. The results are illustrated in Fig. 9, with data presented in the $\varepsilon_a - q$, $p' - q$, $\varepsilon_a - \varepsilon_v$, and $p' - e$ planes. Notably, except for the TX_100 test, the grout specimens displayed contractive behaviour, as evidenced by a decrease in specimen volume during the deviatoric phase (Fig. 9(c)) and a corresponding decrease in void ratio (Fig. 9(d)). Conversely, the TX_100 test exhibited dilative behaviour and a peak in the stress-strain curve (Fig. 9(a)), where the deviatoric stress peaked at approximately 919 kPa before decreasing. This behaviour can be attributed to cementation bonds, as discussed in [11] and in other studies [16–19] of cemented soils. When a specimen is consolidated under high confining stresses (exceeding 100 kPa in this study), the cementation bonds are partly destroyed during isotropic consolidation before shear loading, resulting in more stable (ductile) behaviour. In this state, a limited peak in stress-strain curve is usually seen after an elastic response. In contrast, when consolidated under lower stresses (100 kPa in this study), the cementation bonds remain intact prior to shear loading and break during axial loading, producing a stress-strain curve with a peak corresponding to the peak strength of the cemented bonds (brittle behaviour).

Yield, corresponding to the onset of plastic volumetric strains, can be identified from the discontinuity in the stress-strain curve. Yield corresponds to the start of breakage of the cemented bonds, corresponding to a deconstruction phase as shown in the oedometric tests. In Fig. 10(a), yield is plotted in the $\varepsilon_a - q/p'$ plane as empty dots. The ratio q/p' at yield, $(q/p')_y$, decreases with effective confining stress, as shown in Fig. 10(b). It is noteworthy that the void ratio is consistent with the values obtained in the oedometric tests (Table 3).

Except for the TX_400 test, which was stopped at an axial strain of 12 % due to an experimental issue (temporary loss of power supply in the laboratory), all tests reached a stationary condition in terms of deviatoric stress (Fig. 9(a)) and volumetric strain (Fig. 9 (c)).

Mohr circles representing the final stage of the deviatoric phase are shown in Fig. 11(a), and are used to determine the shear strength envelope. Although the envelope is evidently nonlinear, for the sake of simplicity, the linear Mohr–Coulomb model was used to fit the shear strength envelope. The grout specimens exhibit a cohesion (c') of 111.10 kPa and a shear strength angle (φ') of 35°. Fig. 11(b) shows the failure plane for the TX_500 specimen. As expected, the failure plane has a slope of $45° + \varphi/2$. Good agreement was found among the results of the five tests performed at different effective confining stresses, making it unnecessary to repeat the tests under the same conditions to assess potential discrepancies related to specimen preparation. Moreover, the repeatability of the tests was previously demonstrated in the oedometer experiments (Fig. 6(a), (b)). We also note that there seems to be a relationship between p' and the void ratio in the final stage of the deviatoric phase ($\varepsilon_a \approx 30$ %), as illustrated in Fig. 11(c). Although additional data will be needed to confirm this result, it seems to suggest that at failure, a relationship similar to the critical state line for natural soils may be achieved.

4. Interpretation of laboratory tests

Before proceeding with the interpretation of the results, it is important to highlighted that the bigger part of this study on the 2CG was carried out according to standards that had never been applied to this material before. Consequently, different practical difficulties were encountered and samples tested, in specific conditions, are sometimes limited. Nevertheless, significant insights were obtained, and the following paragraphs describe them in detail.

To determine the yield locus for the grout, the yield points from triaxial tests were plotted in the p'–q plane in Fig. 12(a), along with the failure line, which has a slope $M = 1.40$. The experimental yield points can be fitted by using the equation presented in [20] for fine-grained soils in the framework of critical state soil mechanics:

$$q = -M \bullet p' \bullet \ln\left(\frac{p'}{p'_c}\right) \tag{1}$$

where the parameter p'_c determines the size of the yield locus under isotropic loading conditions. From the triaxial test data, p'_c is found to be 1850 kPa, as shown in Fig. 12(a).

Since this yielding function was used for the original Cam Clay model, it is marked as CC (Cam Clay) in Fig. 12(a).

Specimens under stress states within the yield locus exhibit elastic behavior; when the yield locus is reached, it is assumed that the

Table 4
Results of drained triaxial tests.

Test	e_0	w (%)	σ'_c (kPa)	$e_{post\text{-}cons}$
TX_100	7.798	271	100	7.752
TX_300	7.854	269	300	7.017
TX_400	7.439	266	400	7.366
TX_500	7.518	264	500	7.141
TX_800	7.763	278	800	6.408

e_0=void ratio after preparation; $e_{post\text{-}cons}$=void ratio after consolidation.

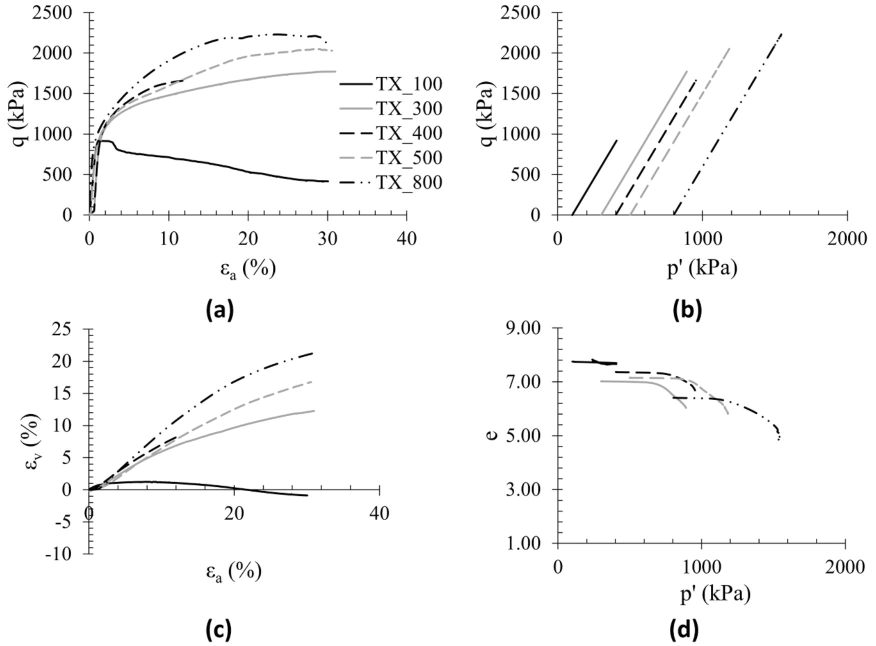

Fig. 9. Results of drained triaxial tests, shown in the (a) ε_a – q, (b) p' – q, (c) ε_a – ε_v, and (d) p' – e planes.

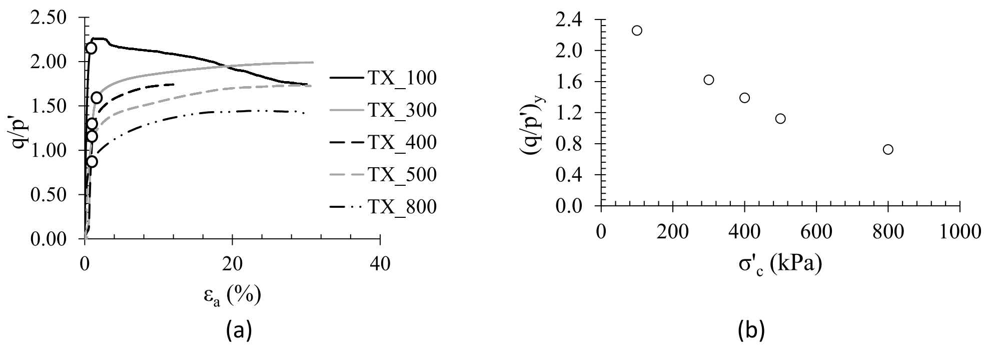

Fig. 10. (a) Identification of yield points (empty dots) in the ε_a – q/p′ plane, and (b) ratio q/p' at yield versus σ'_c.

breakdown of cemented bonds begins, leading to the deconstruction of the grout, as also clearly observed in oedometric conditions.

To compare the data obtained from oedometric tests with those from triaxial tests, the oedometer data were converted to p′ and q values using the following equations:

$$p' = \frac{\sigma'_v \bullet (1 + 2 \bullet K_0)}{3} \tag{2}$$

$$q = p' \bullet \frac{3 \bullet (1 - K_0)}{(1 + 2 \bullet K_0)} \tag{3}$$

where K_0 is the coefficient of earth pressure at rest, which can be estimated using Jacky's formula (K_0=1 − senφ′) and is found to be 0.42 (for φ'=35°; see Fig. 11a). The yield points from the oedometric tests lie on the K_0-line, and the yield point obtained from the oedometric test with a void ratio of seven is plotted in Fig. 12(a). It should be specified that p′ was calculated using Eq. (2) with σ'_v set equal to the deconstruction value of the vertical stress (see the equation in Fig. 7).

Although the yield point obtained from the oedometric test is slightly below the experimental value obtained from the triaxial tests, with an average void ratio of seven, it can be concluded that a single yield locus can be identified. Lower void ratios correspond to higher deconstruction vertical stresses (Fig. 7), which in turn affect the size of the yield locus, causing it to expand.

Fig. 12(b) illustrates the impact of the initial void ratio on the yield locus. As an example, the yield locus was calculated for void ratios of five and three. As the void ratio increases, the elastic field also expands.

These findings are significant for modelling purposes, as they indicate that the behaviour of grout follows critical state soil

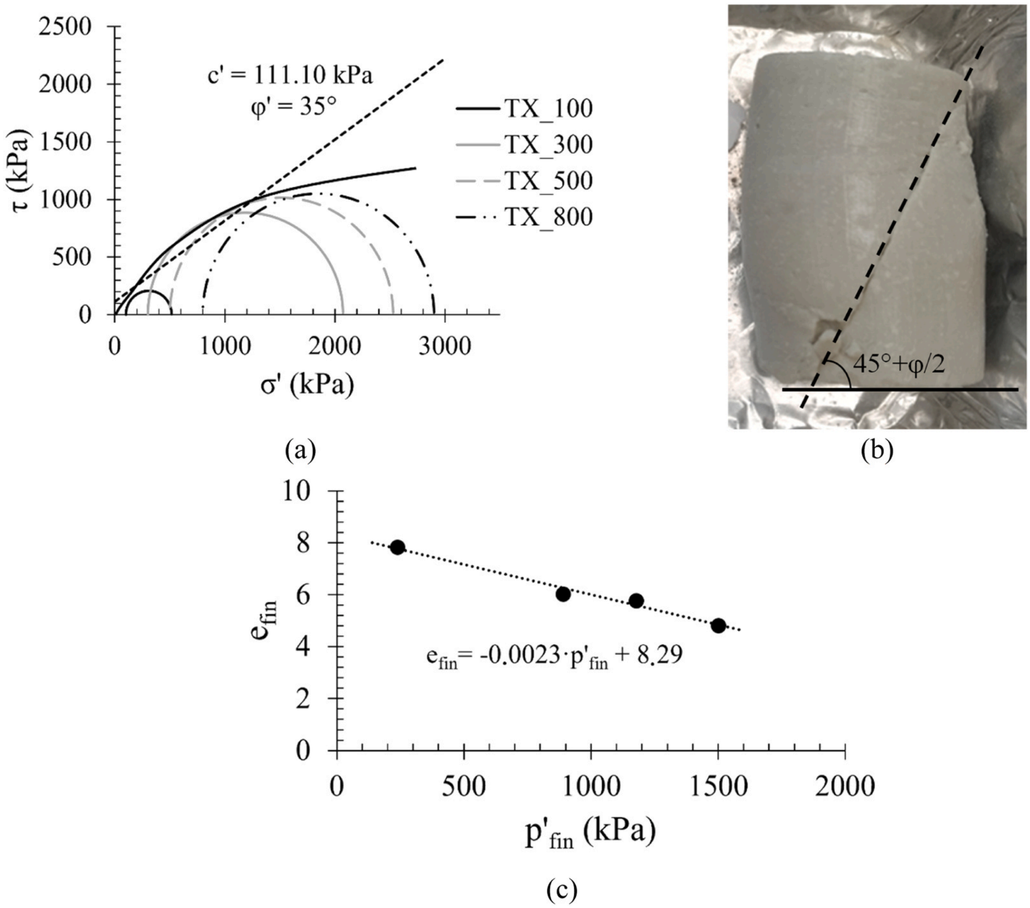

Fig. 11. (a) Mohr's circles and failure envelope for grout specimens, (b) photograph showing failure of specimen TX_500, (c) void ratio versus p′ in the final stage of the deviatoric phase.

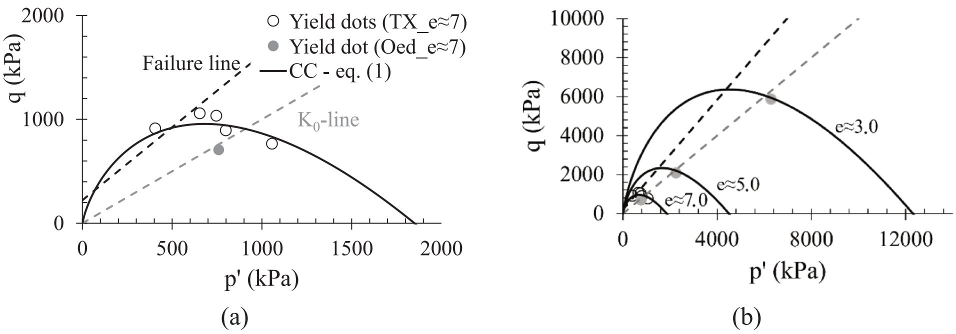

Fig. 12. (a) Experimental yield points and (b) interpolated CC yielding function.

mechanics (CSSM). The authors believe that CSSM can be applied successfully to 2CG for a curing time close to 28 days. Indeed, despite the chemically active nature of 2CG, the cement-base material can be considered ripe after about 1 month of curing (no more chemically active) and consequently the critical state approach could be reasonably applied as already done for cemented soils [16;19].

However, it is a due to remark once again that the analysis is based on few data points and that further laboratory tests would need to be performed to confirm this.

5. Practical considerations for tunnelling

Waterproofing of the segmental lining is of the utmost importance for tunnel performance and maintenance. The value of the grout permeability coefficient (k) was found to be on the order of 10^{-8} cm/s, confirming the suggestion in the technical literature (in most cases without clearly measured evidence) that 2CG is a material that effectively improves the gasket-lining system to achieve the desired level of tunnel waterproofing. It is also important to note that k always has the same order of magnitude, irrespective of the pre-loading applied or the curing times. This finding is of paramount importance, since it can be speculated that if backfilling is correctly performed (with no macroscopic voids left), its waterproofing capacity will be maintained even if subjected to compression loading.

Furthermore, pre-loading has a direct effect on the mechanical properties that can be achieved by the hardened 2CG. From Fig. 7, it can be seen that if a certain pre-load is applied to the material, the consequent reduction in the void ratio improves the final properties of the grout in terms of E_{oed} (Fig. 8). It can be assumed that upon ejection, 2CG has a void ratio of approximately 7.5 (see Tables 3 and 4). When subjected to compressive stresses due to preloading at the curing stage, its void ratio significantly decreases, thereby increasing the deconstruction stress (see Figs. 7 and 12(b)) and enhancing the E_{oed}. Moreover, for a certain level of applied pre-load, a fresher grout gives a higher increase in the constrained modulus, E_{oed}. This aspect should be considered during the assembly phase of the rings in full-face mechanised tunnelling. Indeed, by completing the assembly within a short time, a stiffer backfilling material would be guaranteed in the long term. However, the reduction in volume due to pre-loading needs further investigation, since it could affect the complete filling of the annulus. This aspect should not be underestimated since it could have direct impact on practical aspects in construction site (surface subsidence or lining movements). Notwithstanding that further information are needed, at the present state of the research the authors suggest to slightly increase the injected volume of the backfilling grout during the machine advancement overcoming the usual tolerance of 10–20 % computed on the theoretical volume. Alternatively, the injection pressure refuse threshold could also be increased.

Triaxial testing has been presented in this paper as a valid alternative to direct shear tests for assessing the shear strength of 2CG at long curing times (28 days or longer), although it is important to highlight the discrepancy in the outcomes found using the different methods (Table 5).

Although the failure envelope for the grout is nonlinear, as observed in Section 3.2, the data available in the whole stress range were linearly interpolated, both for the triaxial tests and for the direct shear tests. For long curing times (according to the authors of [21], the material can be considered ripe after 28 days of curing) the values of c' and φ' obtained from the triaxial tests were respectively 60 % and 15 % lower than those obtained from direct shear tests.

These discrepancies are not unexpected, since kinematic constraints affect the shear strength in a direct shear box [22–26], where failure is forced to occur on a predetermined shear plane (horizontal). This restriction leads to higher mobilisation of shear resistance and thus higher values of the shear strength parameters. In contrast, the specimens in the triaxial tests were allowed to fail along the plane shown in Fig. 11(b), resulting in slightly lower and more conservative shear strength parameters.

6. Conclusion

The 2CG material is nowadays the most used in tunnelling when shielded machines are used. Despite its intensive use, lacks concerning its mechanical and hydraulic characteristics are still present. Outcomes of this research are a first step toward a better understanding of the behaviour of this material and they are summarised in the following.

In regard to the waterproofing ability of 2CG, the permeability coefficient was computed as 10^{-8} cm/s, following the Casagrande approach, from one-dimensional compression tests.

Evidence from the compression tests also showed that the load applied at the curing stage of the grout may increase its stiffness. This is due to a reduction in the void ratio upon pre-loading, which seems to be a more critical factor controlling stiffness than the curing time itself for the conditions tested.

Indeed, for the mix design studied here, experimental evidence shows that the oedometric modulus does not have a unique value for a certain curing time; instead, it varies with the applied pre-load, hence the achieved "initial" void ratio. In particular, specimens with lower void ratio, regardless of the curing time tend to exhibit higher E_{oed} than others with higher void ratios. Thus, it can be said that E_{oed} is therefore dependent on the type and quality of the machine injection system. The outcomes reported in this work give values for E_{ed} of about 1 and 2 MPa for samples cured for 1 h (for pre-loads of 100 and 1200 kPa, respectively), about 40 and 9 MPa for samples cured for 1 day (for pre-loads of 100 and 2500 kPa, respectively), and an average value of close to 8 MPa for samples cured for 7 days (for a pre-load of 2500 kPa).

The study also provided shear strength Mohr–Colomb parameters from triaxial tests, which have been never previously carried out for 2CG. These outcomes, in terms of effective cohesion and friction angle, can offer important support for tunnelling design. The smaller values achieved in triaxial tests compared to those obtained from direct shear tests suggest that the former may be more

Table 5
Effective cohesion and friction angles obtained from direct shear tests [8] and triaxial tests (this work).

	Direct shear tests	Triaxial tests
c' (kPa)	272	111
φ' (°)	41	35

conservative.

It is also important to note that this study relies on a limited number of tests for some conditions and further research on these topics is recommended. The numerical values provided refer to the specific mix design used for the production of 2CG (Table 2). Although the dosages of standard ingredients used in 2CG production fall within relative narrow ranges, by changing the mix design (every construction site has its own specific one) variation on numerical results may occur. Concluding, it is strongly recommended to interpret the outcomes of this research by considering the order of magnitude of the numerical values and the trend of the curves from data interpolation. Once stated the limitations, overall, it was possible to attempt a preliminary interpretation of the mechanical behaviour of the 2CG in the framework of CSSM. This lays the foundation for more advanced modelling of such materials in design analyses.

CRediT authorship contribution statement

Lucia Mele: Writing – review & editing, Writing – original draft, Visualization, Methodology, Investigation, Formal analysis, Data curation, Conceptualization. **Carmine Todaro:** Writing – review & editing, Writing – original draft, Resources, Methodology, Investigation, Conceptualization. **Emilio Bilotta:** Writing – review & editing, Validation, Supervision, Data curation. **Daniele Peila:** Writing – review & editing, Supervision, Data curation.

Declaration of Competing Interest

The authors declare that they have no known competing financial interests or personal relationships that could have appeared to influence the work reported in this paper.

Acknowledgements

The authors wish to thank Utt Mapei for providing chemical ingredients, and Buzzi Unicem for providing the cement.

Data Availability

Data will be made available on request.

References

[1] M. Thewes, C. Budach, Grouting of the annular gap in shield tunneling—an important factor for minimisation of settlements and production performance, Proc. Itaaites World Tunn. Congr. (2009).
[2] P. Grasso, A. Lavagno, G. Brino, M. Cardu, D. Martinelli, C. Todaro, A. Carigi, G. Cotugno, D. Peila, M. Concilia, S. Bechter, M. Bringiotti, D. Nicastro, V. Manassero, T. Peinsitt, S. Santarelli, in: E. Bilotta, R. Casale, C.G. di Prisco, S. Miliziano, D. Peila, A. Pigorini, E.M. Pizzarotti (Eds.), Chapter 2 of Handbook on Tunnels and Underground Works: Volume 2: Construction—Methods, Equipment, Tools and Materials, CRC Press, Boca Raton, London, New York, 2023, pp. 11–216, https://doi.org/10.1201/9781003306467-2 (Leiden).
[3] L. André, C. Bacquié, G. Comin, R. Ploton, D. Achard, L. Frouin, M. Cyr, Improvement of two-component grouts by the use of ground granulated blast furnace slag, Tunn. Undergr. Space Technol. 122 (2022) 104369, https://doi.org/10.1016/j.tust.2022.104369.
[4] C. Schulte-Schrepping, R. Breitenbücher, Two-component grouts with alkali-activated binders, in: D. Peila, G. Viggiani, T. Celestino (Eds.), Tunnels and Underground Cities: Engineering and Innovation Meet Archaeology, Architecture and Art, CRC Press, 2019, pp. 3078–3085, https://doi.org/10.1201/9780429424441-326.
[5] C. Todaro, L. Peila, A. Luciani, A. Carigi, D. Martinelli, A. Boscaro, Two component backfilling in shield tunneling: laboratory procedure and results of a test campaign, ITA WTC World Tunn. Congr. Naples (IT) (2019), https://doi.org/10.1201/9780429424441-340.
[6] C. Todaro, M. Bongiorno, A. Carigi, D. Martinelli, Short term strength behavior of two-component backfilling in shield tunneling: comparison between standard penetrometer test results and UCS, Geoing. Ambient. Min. 159 (1) (2020) 33–40.
[7] C. Todaro, F. Pace, Elastic properties of two-component grouts at short curing times: The role of bentonite, Tunn. Undergr. Space Technol. 130 (2022) 104756, https://doi.org/10.1016/j.tust.2022.104756.
[8] C. Todaro, A. Carigi, D. Martinelli, D. Peila, Study of the shear strength evolution over time of two-component backfilling grout in shield tunnelling, Case Stud. Constr. Mater. 15 (2021) e00689, https://doi.org/10.1016/j.cscm.2021.e00689.
[9] ASTM D 854, Standard test methods for specific gravity of soil solids by water pycnometer. Annual Book of ASTM Standards, American Society for Testing and Materials, West Conshohocken, PA, 2023.
[10] ASTM, D 2435, Standard test methods for one-dimensional consolidation properties of soils using incremental loading. Annual Book of ASTM Standards, American Society for Testing and Materials, West Conshohocken, PA, 2011.
[11] C. Oggeri, P. Oreste, G. Spagnoli, The influence of the two-component grout on the behaviour of a segmental lining in tunnelling, Tunn. Undergr. Space Technol. 109 (2021) 103750, https://doi.org/10.1016/j.tust.2020.103750.
[12] ASTM D 7181, Standard test method for consolidated drained triaxial compression test for soils. Annual Book of ASTM Standards, American Society for Testing and Materials, West Conshohocken, PA, 2011.
[13] C. Todaro, A. Godio, D. Martinelli, D. Peila, Ultrasonic measurements for assessing the elastic parameters of two-component grout used in full-face mechanized tunnelling, Tunn. Undergr. Space Technol. 106 (2020) 103630, https://doi.org/10.1016/j.tust.2020.103630.
[14] A. Casagrande, The determination of the pre-consolidation load and its practical significance, Proc. 1st Int. Conf. Soil Mech. (1936) 3–60.
[15] R. Shah, A. Lavasan, D. Peila, C. Todaro, A. Luciani, T. Schanz, Numerical study on backfilling the tail void using a two-component grout, J. Mater. Civ. Eng. 30 (3) (2018) 04018003, https://doi.org/10.1061/(ASCE)MT.1943-5533.000217.
[16] M.R. Coop, J.H. Atkinson, The mechanics of cemented carbonate sands, Geotechnique 43 (1) (1993) 53–67.
[17] B.D. Collins, N. Sitar, Geotechnical properties of cemented sands in steep slopes, J. Geotech. Geoenviron. Eng. 135 (10) (2009) 1359–1366.
[18] A. Hamidi, M. Hooresfand, Effect of fiber reinforcement on triaxial shear behavior of cement treated sand, Geotext. Geomemb 36 (2013) 1–9.
[19] P. Jafarpour, R.Z. Moayed, A. Kordnaeij, Behavior of zeolite-cement grouted sand under triaxial compression test, J. Rock. Mech. Geotech. Eng. 12 (1) (2020) 149–159.
[20] K.H. Roscoe, A. Schofield, A. Thurairajah, Yielding of clays in states wetter than critical, Geotechnique 13 (3) (1963) 211–240.

[21] C. Todaro, A. Godio, D. Martinelli, D. Peila, Ultrasonic measurements for assessing the elastic parameters of two-component grout used in full-face mechanized tunnelling, Tunn. Undergr. Space Technol. 106 (2020) 103630, https://doi.org/10.1016/j.tust.2020.103630.
[22] M.J. Hvorslev, Physical components of the shear strength of saturated clays, Research Conference on Shear Strength of Cohesive Soils, Boulder, Colorado (1960).
[23] P.W. Rowe, The stress-dilatancy relation for static equilibrium of an assembly of particles in contact, Proc. R. Soc. A 269 (1962) 500–527.
[24] P.W. Rowe, The relation between the shear strength of sands in triaxial compression, plane strain and direct shear, Géotechnique 19 (1) (1969) 75–86.
[25] K.H. Bell, The influence of a fixed failure plane on the direct shear test Master's Thesis, University of Missouri at Rolla, 1967.
[26] R. Lancellotta, Geotechnical Engineering, CRC Press, Balkema, Rotterdam, 1993.